https://doi.org/10.5194/egusphere-2026-6329
Preprint. Discussion started: 10 November 2026
© Author(s) 2026. CC BY 4.0 License.

Measurement report: Variability in ambient BVOC compositions along a latitudinal transect of Chinese forests

Di Liu[1], Jianqiang Zeng[2], Hua Fang[2,a], Zhenfeng Wu[2], Shaoxuan Xiao[2], Junjun Deng[3], Pingqing Fu[3], Yanli Zhang[2,4,*], Ping'an Peng[2], Xinming Wang[2,4,*]

[1]School of Environment, Beijing Normal University, Beijing 100875, China

[2]State Key Laboratory of Advanced Environmental Technology and Guangdong Key Laboratory of Environmental Protection and Resources Utilization, Guangzhou Institute of Geochemistry, Chinese Academy of Sciences, Guangzhou 510640, China

[3]Institute of Surface-Earth System Science, School of Earth System Science, Tianjin University, Tianjin, 300072, China

[4]College of Resources and Environment, University of Chinese Academy of Sciences, Beijing 100049, China

Correspondence to: Yanli Zhang (zhang_yl86@gig.ac.cn) and Xinming Wang (wangxm@gig.ac.cn)

[a]Now at School of Ecology and Environment, Anhui Normal University, Wuhu 241000, China

Abstract. Forest biogenic volatile organic compounds (BVOCs) affect oxidant cycling and secondary pollution, but coordinated observations of speciated ambient BVOCs remain scarce across China's diverse forests, limiting the evaluation of regional models. We measured ambient isoprene, monoterpenes (MTs), and sesquiterpenes (SQTs) at eight sites spanning tropical to cold-temperate China using a common cartridge-based thermal-desorption gas chromatography-mass spectrometry protocol. We collected ambient samples during summer at all sites and winter at five sites, using fixed daytime and nighttime sampling windows. Summer mean mixing ratios ranged from 30 to 709 ppt for isoprene, 129 to 470 ppt for MTs, and 11 to 27 ppt for SQTs. Isoprene dominated the BVOC mixture at most broadleaf sites, whereas MTs were more prominent at the needleleaf and shrub-steppe sites. Winter concentrations tended to be lower at paired sites, but the seasonal comparison was not significant. Summer daytime isoprene concentrations were higher at all sites. Five sites showed positive associations between daytime, ln-transformed isoprene and air temperature, whereas three sites showed no significant fit. The summer MT day-to-night proxy ratio decreased significantly with latitude. Concentration-weighted metrics indicated that isoprene dominated daytime OH reactivity and ozone formation at broadleaf sites, whereas MTs contributed strongly to nighttime nitrate-radical reactivity and secondary organic aerosol formation. Because we measured in ambient air and collected samples in fixed windows, these concentrations and derived potentials do not represent direct emission fluxes or complete atmospheric production. The dataset provides a cross-ecosystem benchmark for evaluating BVOC composition and sampling-period variability in regional atmospheric chemistry models.

https://doi.org/10.5194/egusphere-2026-6329
Preprint. Discussion started: 10 November 2026
© Author(s) 2026. CC BY 4.0 License.

1 Introduction

Forests emit biogenic volatile organic compounds (BVOCs) that participate in atmospheric oxidation, ozone chemistry, secondary organic aerosol formation, and new particle formation (Chameides et al., 1988; Claeys et al., 2004; Curtius et al., 2024; Zhao et al., 2024). The atmospheric roles of these compounds depend not only on their total abundance but also on their chemical composition. Isoprene, monoterpenes (MTs), and sesquiterpenes (SQTs) have different reaction rates and oxidation pathways, and their relative contributions vary among plant communities and forest types (Guenther et al., 2012). Broadleaf forests often have larger isoprene contributions, whereas needleleaf forests can be dominated by MTs. These differences can alter the balance of daytime OH and ozone chemistry, nighttime nitrate-radical chemistry, and organic aerosol formation (Kiendler-Scharr et al., 2009; McFiggans et al., 2019). Resolving BVOC composition across contrasting forest environments is therefore important for evaluating atmospheric chemistry and for developing regionally appropriate emission representations.

BVOC emissions are regulated by interacting environmental and physiological processes (Guenther et al., 1993; Kesselmeier & Staudt, 1999; Niinemets et al., 2004; Laothawornkitkul et al., 2009; Zeng et al., 2023, 2025a). They exhibit high sensitivity to temperature and light, with distinct patterns among major compound classes. Isoprene emission is strongly light-dependent and declines rapidly after dark (Loreto and Sharkey, 1990; Sharkey et al., 2008), whereas MTs and sesquiterpenes (SQTs) can be emitted both de novo (light-dependent) and from storage pools (light-independent), allowing release during both day and night (Staudt and Bertin, 1998; Niinemets et al., 2004; Niinemets et al., 2010; Zeng et al., 2025c). Leaf phenology further regulates emission dynamics: emission potentials are low in new foliage, increase with leaf expansion, peak at maturity, and decline during senescence (Sharkey et al., 2008; Guenther et al., 2012; Gomes Alves et al., 2023). Consequently, seasonal and diurnal variations in temperature and light, combined with phenological alterations, collectively shape the fluxes and blend of BVOCs emitted from forests, thereby influencing their chemical feedback in the atmosphere.

Ambient observations provide a complementary perspective on these controls. Unlike leaf- or canopy-scale flux measurements (Sarkar et al., 2020; Zeng et al., 2022; Zeng et al., 2025c), ambient mixing ratios integrate local emission strength with chemical loss, dilution, transport, and boundary-layer dynamics (Bourtsoukidis et al., 2014; Hellén et al., 2018; Zannoni et al., 2020). They therefore cannot be interpreted as emission fluxes, but they directly constrain the BVOC mixtures encountered by the atmosphere. This distinction is especially important for atmospheric chemistry applications, because the composition and sampling-time dependence of ambient BVOCs determine the compounds available for oxidation and provide an observational basis for evaluating emission inventories and chemical transport models. Ambient observations are more logistically flexible and less equipment-intensive, and they remain essential for evaluating the contribution of BVOCs to ozone and aerosol formation (Jia et al., 2024; Chen et al., 2025) and for constraining regional air quality models (Zhang et al., 2020). This is especially relevant given that bidirectional transport of BVOCs and anthropogenic pollutants between forests and urban areas can significantly influence secondary pollution in both regions (Shrivastava et al., 2019; Wang et al., 2022; Li et al., 2025; Zhang et al., 2026). Although numerous forest ambient BVOC measurements have been conducted worldwide (Bouvier-Brown et al., 2009; Xue et al., 2013; Bourtsoukidis et al., 2014; Hellén et al., 2018; Gong et al., 2018; Gomes Alves et al., 2023; Petersen et al., 2025), most studies are specific to a single site, limiting their utility for evaluating large-scale emission and chemistry frameworks. Coordinated observations are therefore especially useful because single-site campaigns may confound analytical differences with ecosystem and meteorological differences.

China is a particularly important but still incompletely characterized domain for such observations. Its vegetation and climate span tropical, subtropical, temperate, and cold-temperate ecosystems across a broad latitudinal and elevational range (Su et al., 2020). BVOC observations in China are consequently relevant to both regional atmospheric chemistry and the transferability of emission

https://doi.org/10.5194/egusphere-2026-6329
Preprint. Discussion started: 10 November 2026
© Author(s) 2026. CC BY 4.0 License.

parameterizations across contrasting ecosystems. They are also important because biogenic emissions interact with anthropogenic pollution and can influence ozone and aerosol formation beyond the immediate forest environment (Wang et al., 2022; Li et al., 2025). However, the available Chinese record remains fragmented. Existing studies have reported isoprene or selected VOCs at individual mountain and forest sites, while a multi-site network has mainly characterized isoprene rather than a consistently speciated BVOC mixture (Guo et al., 2012; Gong et al., 2018; Zhang et al., 2020). Reviews and regional syntheses further indicate that ambient measurements of MTs and especially SQTs remain much less extensive than measurements of isoprene (Guo et al., 2017; Jia et al., 2024). The scarcity is therefore not simply a shortage of sampling locations. It also concerns the lack of comparable observations across forest types, seasons, sampling times, and compound classes. Without such coordinated measurements, it is difficult to distinguish ecological contrasts from differences in analytical protocol, sampling design, or temporal coverage, and difficult to evaluate whether model parameterizations reproduce the BVOC mixtures that actually occur in the atmosphere over Chinese forests.

To address this gap, we applied an identical sampling and analytical protocol to ambient air at eight sites spanning tropical to cold-temperate forests and adjacent montane shrub-steppe in China. We used a common analyte panel to examine how isoprene, MTs, and SQTs vary among sites and between summer and winter, and we evaluated fixed sampling-time contrasts without treating them as a complete diel cycle. We ask whether coordinated observations reveal systematic spatial, seasonal, and diel organization in ambient BVOC composition across Chinese forest environments, and how these composition patterns affect calculated oxidant reactivities and ozone and secondary organic aerosol formation potentials. Although latitude and forest type are used here as descriptors of the observational gradient rather than as independently identified causal drivers, the resulting dataset, based on synchronous measurements of isoprene, MTs, and SQTs across multiple forest types, provides a comparable ambient benchmark for BVOC speciation and temporal variability, with direct relevance to the evaluation of regional emission inventories and atmospheric chemistry models.

2 Materials and methods

2.1 Study sites and ambient-air sampling

Ambient BVOC measurements were conducted at eight sites spanning tropical to cold-temperate China: Jianfengling (JFL), Xishuangbanna (XSBN), Mt. Wuyi (WYS), Shennongjia (SNJ), the Qinling Mountains (QL), the Qilian Mountains (QLS), Mt. Changbai (CBS), and the Great Khingan Mountains (DXAL). The sites covered 18.738-50.820° N, 100.290-128.107° E and elevations of approximately 570-2561 m above sea level. They represented tropical and subtropical broadleaf forests, temperate broadleaf forests, cold-temperate needleleaf forest, and montane shrub-steppe (Fig. S1 and Table S1).

The summer campaign was conducted at all eight sites from 23 to 28 August 2019. The winter campaign was conducted from 25 to 30 December 2019 at JFL, XSBN, WYS, SNJ, and CBS. QL, QLS, or DXAL were not sampled in winter because of severe cold conditions. All samplers were housed inside the forest protection station buildings. Ambient air was drawn into the sampling cartridges through polytetrafluoroethylene (PTFE) tubing with a length of approximately 3–5 m and an inner diameter of 1/4 inch. The sampling inlet was positioned approximately 3 m above the ground, outside the forest canopy. At each site, ambient air was collected using a JEC921 automatic sampler at 500 mL min^{-1} for 2 h per sample, corresponding to a nominal sample volume of 60 L. Air was drawn through Tenax TA/Carbograph 5TD cartridges. An upstream quartz-fibre filter treated with sodium thiosulfate was used to remove particles and ozone. Prior to field deployment, breakthrough tests were performed in July 2019 at Mt. Huolu (Guangzhou, China) by sampling ambient air through two cartridges connected in series. No target compounds were detected above the method detection limits in the second cartridge, confirming the absence of breakthrough. This is consistent with previous

https://doi.org/10.5194/egusphere-2026-6329
Preprint. Discussion started: 10 November 2026
© Author(s) 2026. CC BY 4.0 License.

studies that reported no breakthrough of VOCs even under high-concentration conditions when using large sampling volumes (Fang et al., 2021a, 2021b).

Summer samples were collected during four clock-time intervals: 09:00-11:00, 13:00-15:00, 17:00-19:00, and 21:00-23:00 (UTC+8). Winter sampling included two additional intervals: 01:00-03:00 and 05:00-07:00. These fixed sampling periods were used to compare observed time-of-day patterns and were not treated as continuous diel measurements. Site-season sample counts are summarized in Table S1. Samples affected by technical problems were excluded. The resulting registry contained 339 quality-controlled 2 h samples: 23 JFL, 22 XSBN, 21 WYS, 17 SNJ, 23 QL, 23 QLS, 21 CBS, and 21 DXAL samples in summer, and 33 JFL, 32 XSBN, 36 WYS, 34 SNJ, and 33 CBS samples in winter.

2.2 Cartridge preparation and analysis

Cartridges were conditioned under nitrogen at 320 °C and checked in batches. Field and pre-campaign tandem-cartridge tests found no target compounds above their method detection limits in the second cartridge. After sampling, cartridges were sealed, transported at 4 °C, stored at -20 °C, and analysed within 10 days.

Cartridges were analysed with a Markes TD-100 thermal-desorption system coupled to an Agilent 7890 gas chromatograph (GC) and 5975 mass-selective detector (MSD). Primary desorption was performed at 280 °C for 10 min, followed by cryofocusing at -10 °C. Compounds were separated on an HP-5MS column (30 m length × 0.25 mm I.D. × 0.25 μm film thickness). The oven was held at 35 °C for 3 min, ramped to 100 °C at 5 °C min^{-1} and held for 1 min, ramped to 120 °C at 10 °C min^{-1} and held for 12 min, and then ramped at 20 °C min^{-1} to 260 °C and held for 2 min. The MSD used 70 eV electron ionization (EI) and full-scan and selected ion monitoring (SIM) modes. Except for the tentatively assigned MT peak described in Sect. 3.2, target compounds were identified by comparing retention times and mass spectra with authenticated standards and quantified with external calibration. Analytical details can be found elsewhere (Zeng et al., 2022, 2023, 2025d). For a nominal sample volume of 60 L, the reported method detection limits (MDLs) were 0.6 ppt for isoprene, 0.11-0.49 ppt for MTs, and 0.06-0.90 ppt for SQTs.

2.3 Calculation of oxidant reactivity and ozone/SOA formation potentials

BVOC-weighted reactivity with oxidant *j* was calculated as

$$R_j = \sum k_{i,j} \times [X]_i \quad (1)$$

where $\boldsymbol{k_{i,j}}$ is the bimolecular rate coefficient for reaction of compound ***i*** with oxidant ***j*** (OH, O_3 or NO_3), and $[X_i]$ is the number concentration of compound i (molecules cm^{-3}). Rate constants are listed in Table S2. For the tentatively assigned α-terpinene peak, α-pinene rate constants were used as surrogates.

Ozone formation potential (OFP) and secondary organic aerosol (SOA) formation potential (SOAFP) were calculated as

$$OFP = \sum MIR_i \times [X]_i \quad (2)$$

$$SOAFP = \sum Y_i \times [X]_i \quad (3)$$

where, in Eq. (2), $[X]_i$ is the measured mixing ratio of compound i in ppb, MIR_i is the maximum incremental reactivity in ppb O_3 per ppb BVOC, and Y_i in Eq. (3) is the SOA yield. The compound-specific MIR values and SOA yields are listed in Table S3; the MIR values have been converted from a mass basis to a molar basis. These metrics are calculated potentials, not measurements of realized ozone or SOA production.

2.4 Data processing and statistical analysis

Summary values are reported as means and standard deviations where indicated in the tables and figure captions. Seasonal

https://doi.org/10.5194/egusphere-2026-6329
Preprint. Discussion started: 10 November 2026
© Author(s) 2026. CC BY 4.0 License.

differences were evaluated at the five sites sampled in both seasons using two-sided Wilcoxon tests. The association between latitude and the summer MT day-to-night proxy ratio was evaluated using Spearman rank correlation across the eight sites (Fig. S14).

https://doi.org/10.5194/egusphere-2026-6329
Preprint. Discussion started: 10 November 2026
© Author(s) 2026. CC BY 4.0 License.

3 Results

3.1 Overview of BVOCs at eight forests

BVOC mixing ratios exhibited highly spatiotemporal heterogeneity (Fig. 1). Spatially during summer, mean isoprene levels ranged between 250 and 750 ppt at most forests, but were 106 ppt at DXAL and below 100 ppt at the Qilian Mts. (Fig. 1a). Summertime MT mixing ratios typically varied between 100 and 500 ppt (Fig. 1a), whereas SQTs were an order of magnitude lower, generally between 10 and 30 ppt (Fig. 1a). Seasonally, mean BVOC mixing ratios were lower in winter than in summer at the five paired sites, but the reported seasonal comparison did not reach the 0.05 significance threshold. Most forests recorded mean winter isoprene levels below 100 ppt, except at JFL where they exceeded 250 ppt (Fig. 1b). Wintertime MT mixing ratios mostly ranged between 25 and 150 ppt, except at CBS where they fell below 10 ppt (Fig. 1b). SQT mixing ratios in winter were largely under 5 ppt, yet JFL averaged 7 ppt (Fig. 1b).

Diurnal patterns differed among compound classes. Isoprene mixing ratios were higher during daytime than nighttime at all sites in summer; winter contrasts were more site-dependent. In contrast, MTs and SQTs displayed more complex, site-dependent diurnal cycles. During summer, MT mixing ratios were higher in daytime at low-latitude sites (e.g., JFL, XSBN, WYS) but lower during the day at higher-latitude forests. In winter, all sites showed lower daytime MT mixing ratios. For SQTs, most forests exhibited lower daytime levels, although a slight daytime increase was observed in summer at WYS and QLS.

3.2 Spatial and seasonal variation in ambient BVOCs

BVOC mixing ratios displayed strong seasonal contrasts, with summer mean values exceeding winter levels for all three compound classes at the five sites sampled in both seasons (Fig. 2, Fig. S2, Table 1). Mean summer mixing ratios ranged from 30 to 709 ppt for isoprene, 129 to 470 ppt for MTs, and 11 to 27 ppt for SQTs. The highest summer isoprene level was observed at the QL (709 ppt), followed by WYS (639 ppt) and CBS (503 ppt), whereas the Qilian Mts. showed the lowest (30 ppt). For MTs, the DXAL recorded the maximum (470 ppt), ahead of WYS (329 ppt) and CBS (261 ppt). SQTs were highest at WYS (27 ppt), then JFL (20 ppt) and the DXAL (19 ppt). In winter, BVOC mixing ratios declined markedly (Table 1). Mean isoprene ranged from 43 to 289 ppt, with only JFL exceeding 100 ppt (289 ppt). MTs ranged between 8 and 131 ppt, peaking at WYS, while other forests remained below 60 ppt. SQTs were mostly below 5 ppt, except at JFL (7 ppt). Consequently, summer-to-winter ratios varied widely: 1.4-23.4 for isoprene, 3.1-48.8 for MTs, and 2.0-16.4 for SQTs.

Chemically, isoprene dominated (63-81%) the summertime BVOC mixture at most forests, except at the Qilian Mts. and the DXAL, where MTs contributed 76% and 79%, respectively (Fig. S3). In winter, isoprene remained the major component (60-83%) at most sites, whereas MTs predominated at WYS (72%). The fractional contribution of SQTs remained below 6% in all seasons. Although MT mixing ratios changed seasonally, their compositional profiles were relatively stable (Fig. 3). Twelve components were reported in the summer MT group across the eight sites, including α-pinene, camphene, β-pinene, β-myrcene, limonene, 3-carene, α-phellandrene, 1,8-cineole, γ-terpinene, terpinolene, linalool, and one unidentified MT tentatively assigned as α-terpinene based on literature reports (Yáñez-Serrano et al., 2018; Mermet et al., 2019). Excluding the Qilian Mts., five common MTs (α-pinene, camphene, β-pinene, β-myrcene, and limonene) collectively accounted for >85% of total MTs in both seasons (Fig. 3a and c; Figs. S4 and S5). Dominant MT speciation, however, varied by site. In summer, α-pinene was most abundant at WYS (37%, 120 ppt), SNJ (38%, 49 ppt), the QL (41%, 61 ppt), and the DXAL (29%, 136 ppt); β-pinene dominated at JFL (39%, 67 ppt) and XSBN (42%, 69 ppt); and camphene was predominant at CBS (33%, 86 ppt). At the Qilian Mts., these five MTs contributed 55%, while the possible α-terpinene represented the largest proportion (38%).

In contrast, both the mixing ratios and composition of SQTs showed distinct seasonal shifts (Fig. 3b and d; Fig. S6). Six SQTs

https://doi.org/10.5194/egusphere-2026-6329
Preprint. Discussion started: 10 November 2026
© Author(s) 2026. CC BY 4.0 License.

were detected in summer: α-longipinene, longicyclene, β-caryophyllene, thujopsene, aromadendrene, and alloaromadendrene. In winter, only two to four of them were detected, with markedly lower mixing ratios. Longicyclene was the most abundant SQT in summer at XSBN (33%, 4.0 ppt), WYS (34%, 9.0 ppt), and the Qilian Mts. (47%, 5.2 ppt); α-longipinene dominated at SNJ (29%, 4.4 ppt), CBS (32%, 3.4 ppt), and the DXAL (27%, 5.3 ppt); β-caryophyllene showed the highest proportion at JFL (48%, 9.8 ppt); and alloaromadendrene was predominant at the QL (27%, 3.9 ppt). During winter, all SQT mixing ratios were below 3 ppt, with β-caryophyllene detected across all forests.

3.3 Diurnal patterns

Diurnal patterns of BVOC mixing ratios varied across forest sites (Fig. 4). During summer, isoprene consistently showed higher mixing ratios during daytime at all forests, with the highest sampled-period means occurring at 13:00-15:00 or 17:00-19:00 (UTC+8) (Fig. S7). The highest daytime summer isoprene level was observed at the QL (862 ppt), followed by WYS (847 ppt) and CBS (659 ppt). In winter, this daytime enhancement persisted only in low-latitude tropical forests (JFL and XSBN), while other sites exhibited minimal diurnal variation (Fig. S8). MTs displayed more complex, forest-dependent diurnal cycles (Fig. 4). In summer, low-latitude forests (e.g., JFL, XSBN, and WYS) showed higher daytime MT mixing ratios, correlating positively with isoprene. In contrast, higher-latitude forests exhibited elevated nighttime MT levels, inversely related to isoprene. The highest average daytime MT mixing ratio in summer was recorded at WYS (345 ppt), followed by the DXAL (316 ppt); all other forests remained below 200 ppt (Fig. S9). At night, the highest MT levels occurred at the DXAL (828 ppt), with CBS (599 ppt) and the QL (378 ppt) following. In winter, most forests, including those at low latitudes, displayed higher MT mixing ratios at night, with averages generally below 100 ppt for both day and night (Fig. S11).

Most forests also exhibited higher SQT mixing ratios at night during summer, except for WYS and the Qilian Mts., where daytime levels were higher (Fig. 4). The sampling-period pattern of SQTs differed from that of MTs across sites, without identifying the underlying emission controls. SQT mixing ratios correlated positively with isoprene at WYS and the Qilian Mts., but negatively elsewhere (Fig. S10). The highest average daytime SQT mixing ratio in summer occurred at WYS (26 ppt), followed by JFL (17 ppt) and the DXAL (13 ppt). The highest nighttime level was observed at the DXAL (35 ppt), then SNJ (23 ppt), with WYS and the QL both at 20 ppt (Fig. S9). In winter, SQT mixing ratios were low overall (<5 ppt), except at JFL where the nighttime mean reached 8 ppt (Fig. S11).

During summer, positive linear associations between logarithmically transformed daytime isoprene mixing ratios and air temperature were significant at JFL, WYS, QL, and CBS (Fig. S12). A borderline association was shown at DXAL ($p = 0.05$), whereas no significant fits were evident at XSBN, SNJ, or QLS. These ambient patterns are consistent with temperature-responsive isoprene emission functions in established models and branch-scale observations from southern China (Guenther et al., 1993, 2012; Zeng et al., 2023). However, ambient concentration-temperature associations do not isolate emission responses from covarying light, transport, mixing, or chemical loss.

3.4 Calculated oxidant reactivities and formation potentials

Calculated BVOC-weighted oxidant reactivities were substantially higher in summer than in winter (Fig. 5). During summer, OH reactivity (R_{OH}) remained below 4 s^{-1} across all forests and times, NO_3 reactivity (R_{NO3}) was below 0.2 s^{-1}, and O_3 reactivity (R_{O3}) was below 6×10^{-6} s^{-1}. Mean daytime R_{OH} across the eight forests ranged from 0.33 to 2.75 s^{-1}, with the highest at WYS (2.75 s^{-1}), followed by the QL (2.38 s^{-1}) and CBS (2.01 s^{-1}). The maximum R_{OH} was also observed at WYS (3.73 s^{-1}). Mean daytime R_{O3} in summer ranged from 0.84 to 3.63×10^{-6} s^{-1}, peaking at JFL (3.63×10^{-6} s^{-1}). Nighttime R_{O3} (1.64-5.57×10^{-6} s^{-1}) exceeded daytime levels, and the top three were CBS (5.57×10^{-6} s^{-1}), the DXAL (4.35×10^{-6} s^{-1}), and SNJ (3.34×10^{-6} s^{-1}). Nighttime R_{NO3} varied from

https://doi.org/10.5194/egusphere-2026-6329
Preprint. Discussion started: 10 November 2026
© Author(s) 2026. CC BY 4.0 License.

0.02 to 0.17 s^{-1}, with the highest three being CBS (0.17 s^{-1}), the DXAL (0.16 s^{-1}), and SNJ (0.07 s^{-1}).

In winter, reactivities declined markedly due to lower BVOC mixing ratios. Most R_{OH} values fell below 1 s^{-1}, R_{NO3} below 0.025 s^{-1}, and R_{O3} below 1×10^{-6} s^{-1}. Except for JFL where mean daytime R_{OH} was 1.18 s^{-1}, all other forests had values below 0.5 s^{-1}. Daytime R_{O3} was highest at JFL (1.14×10^{-6} s^{-1}) and below 0.5×10^{-6} s^{-1} elsewhere. The top three forests for nighttime R_{O3} were JFL (0.62×10^{-6} s^{-1}), XSBN (0.45×10^{-6} s^{-1}), and WYS (0.35×10^{-6} s^{-1}). Nighttime R_{NO3} in winter was also highest at these three sites: WYS (0.022 s^{-1}), JFL (0.016 s^{-1}), and XSBN (0.010 s^{-1}).

The site-wise contribution summaries showed distinct roles for the BVOC classes (Figs. S15 and S16). At broadleaf sites, isoprene supplied 65-89% of calculated OH reactivity. At QLS and DXAL, MTs contributed 68% of OH reactivity at each site. MTs accounted for 66-97% of nighttime R_{NO3} across the sampled sites. MTs and SQTs together supplied at least 80% of R_{O3}. At broadleaf sites, isoprene contributed 72-93% of calculated OFP values. MTs instead contributed 70% at QLS and 61% at DXAL. Across the sites, MTs accounted for 74-91% of calculated SOAFP. It is worth noting that these percentages describe the composition of calculated potentials, not measured ozone production or aerosol formation. Calculated OFP and SOAFP values for summer and winter are shown in Fig. 6.

4 Discussion

4.1 A coordinated ambient benchmark across contrasting forests

The coordinated measurements provide a comparable, speciated ambient BVOC benchmark across eight Chinese forest and montane ecosystems. This complements the fragmented Chinese observational record, in which measurements have often focused on individual sites or on a narrower set of compounds. The value of this dataset is therefore not a single site ranking, but the comparison of isoprene, monoterpenes (MTs), and sesquiterpenes (SQTs) under a common sampling and analytical protocol.

Most of our observed summertime site-mean isoprene mixing ratios, except at QLS, fall within the broad range (100-1,120 ppt) reported for twenty urban and regional sites across China (Zhang et al., 2020), while two tropical forest sites had lower mixing ratios than several tropical Asian and Amazonian studies, in which isoprene exceeded 1,000 ppt and could reach over 6,000 ppt (Jones et al., 2011; Sarkar et al., 2020; Gomes Alves et al., 2023; Table S4). Similarly, MT mixing ratios at our tropical sites (172 ppt at JFL and 164 ppt at XSBN) were modest relative to other rainforest studies. These comparatively low values may reflect several factors: our samples were collected outside the forest canopy, allowing atmospheric oxidation during transport, and inherent variability in BVOC emission potentials and plant species composition among forests likely also plays a role (Batista et al., 2019).

In subtropical broadleaf forests, the mean isoprene mixing ratio at WYS (639 ppt) exceeded values reported from Mt. Tian Jing (287 ppt; Gong et al., 2018) and Mt. Tai Mo Shan (109 ppt; Guo et al., 2012). Temperate broadleaf forests in our study (286-709 ppt) showed isoprene levels comparable to earlier reports (152-753 ppt; Table S4). Consistent with needleleaf forests being strong MT emitters, DXAL exhibited higher MT levels (470 ppt) than isoprene (106 ppt), aligning with previous needleleaf forest observations (Ramasamy et al., 2016; Petersen et al., 2025; Table S4). Grass- and shrublands, which generally have lower BVOC emission capacities, displayed lower mixing ratios than most woody forests (Table 1; Table S4). Summertime SQT mixing ratios (11-27 ppt) across our sites were also consistent with the range of prior measurements (Table S4).

4.2 Seasonal contrasts and compositional stability

At the five sites sampled in both seasons, mean concentrations of the measured BVOC classes were substantially lower in winter. Seasonal changes in temperature and leaf phenology provide plausible explanations for part of the observed contrasts. These controls on BVOC emissions have been documented in previous studies (Kuhn et al., 2004; Gomes Alves et al., 2023; Zeng et al.,

https://doi.org/10.5194/egusphere-2026-6329
Preprint. Discussion started: 10 November 2026
© Author(s) 2026. CC BY 4.0 License.

2025a). Across the five paired sites, the summer-to-winter BVOC ratios covaried positively with the seasonal temperature difference (Fig. S13). Lower winter temperatures reduce the production, volatilization, and diffusion of BVOCs (Laothawornkitkul et al., 2009), while phenological controls, such as the timing of bud break, leaf expansion, maturation, and senescence, further modulate emission fluxes (Sharkey et al., 2008; Guenther et al., 2012; Gomes Alves et al., 2023). These processes may contribute to the lower winter mixing ratios, but their effects cannot be separated here from seasonal changes in atmospheric mixing, transport, and chemical loss (Fig. 2).

Despite the overall decline in wintertime mixing ratios, the compositional profile of MTs remained relatively stable across most forests. This similarity in ambient composition does not distinguish seasonal changes in emissions from species-dependent atmospheric processing. Notably, five common MTs (α-pinene, camphene, β-pinene, β-myrcene, and limonene) accounted for >85 % of total MTs at the sites other than QLS, in agreement with previous observations across diverse forest types (Hellén et al., 2018; Yáñez-Serrano et al., 2018; Petersen et al., 2025) and with global model representations (Guenther et al., 2012). In contrast, both the mixing ratios and the number of detected SQT species decreased markedly in winter, consistent with temperature-sensitive SQT emissions (Duhl et al., 2008; Ortega et al., 2008). The smaller number of detected species must also be interpreted in relation to the method detection limits.

4.3 Diurnal variation and controls

Our results revealed distinct diurnal patterns among BVOC classes. Isoprene showed higher daytime mixing ratios at all sites in summer, whereas MTs exhibited contrasting patterns across sites: JFL, XSBN, and WYS displayed higher daytime mixing ratios, while higher-latitude forests showed elevated nighttime levels. Although related sampling-time patterns have been reported at individual forest sites (Hellén et al., 2018; Sarkar et al., 2020; Petersen et al., 2025), our multi-site observations provide a synchronous comparison of ambient MT concentration patterns along the sampled latitudinal transect.

Daytime regressions provide additional, but spatially variable, evidence of an association between air temperature and isoprene mixing ratios (Fig. S12). Positive fits at four sites and a borderline fit at DXAL are consistent with temperature responses represented in emission algorithms (Guenther et al., 1993, 2012). Branch-scale measurements in southern China also support temperature-responsive isoprene emissions (Zeng et al., 2023). The absence of significant fits at XSBN, SNJ, and QLS cautions against treating air temperature as a uniform predictor across these forests. Because these regressions relate ambient mixing ratios to air temperature, they cannot isolate temperature-driven emissions from covarying light, canopy mixing, transport, or chemical loss.

Diurnal variations in ambient mixing ratios are governed by emission strength, chemical loss, and boundary layer dynamics. Previous studies have shown that vertical mixing strongly affects MT concentrations at a boreal forest site (Hellén et al., 2018), whereas light-dependent MT emissions have been observed in an Amazonian forest (Sarkar et al., 2020). At a Scandinavian boreal forest, MT and SQT concentrations generally peaked at night, whereas the measured terpene fluxes generally peaked around noon (Petersen et al., 2025). In this study, the four sampling-period means showed positive MT–isoprene covariation at lower-latitude sites and negative covariation at higher-latitude sites (Fig. 4). Because isoprene emission is strongly light-dependent, its nocturnal decline is consistent with reduced emissions, although atmospheric mixing and chemical loss also influence ambient concentrations. These contrasting concentration patterns are compatible with contributions from light-independent MT emissions, but do not determine their relative importance or establish a latitudinal change in emission light dependence.

SQTs did not follow the same sampling-period pattern across sites as MTs. Previous studies indicate that SQT emissions can include light-dependent and light-independent components (Duhl et al., 2008; Zeng et al., 2025c). At WYS and the QLS, SQT

https://doi.org/10.5194/egusphere-2026-6329
Preprint. Discussion started: 10 November 2026
© Author(s) 2026. CC BY 4.0 License.

mixing ratios correlated positively with isoprene. In other forests, including tropical sites, SQT mixing ratios were negatively correlated with isoprene. Nevertheless, quantifying the light dependencies of MT and SQT emissions will require further leaf- or branch-scale experimental constraints.

4.4 Implications for atmospheric chemistry

Our measurements constrain the calculated OH reactivity of the measured isoprenoids (isoprene, MTs, and SQTs), rather than total ambient OH reactivity. Daytime isoprenoid R_{OH} in this study ranged from 0.33 to 2.75 s^{-1}, lower than most of the calculated biogenic-compound reactivities compiled from other forest studies in Table S5 (Fig. 5c). Observed total OH reactivities from other forests are compiled separately in Table S6. Because our samples were collected in ambient air near, rather than within, the canopy and our measurements covered only a subset of reactive organics, this comparison should be interpreted in light of differences in sampling conditions and compound coverage, rather than as a direct OH reactivity closure assessment. Without co-located measurements of total OH reactivity, neither the magnitude nor the sources of unaccounted reactivity at our sites can be determined.

Despite that limitation, the coordinated dataset provides useful information for simplifying and evaluating BVOC speciation in models. In the broadleaf forests, isoprene dominated BVOC-related R_{OH} and daytime OFP, contributing 65-89 % of the calculated R_{OH} and more than 70 % of sunlit OFP, whereas MTs dominated the shrub-grassland and needleleaf sites. Moreover, five MTs accounted for more than 85 % of total MTs at most forests. Together, these patterns suggest that a relatively compact MT speciation framework, combined with forest-type-dependent partitioning between isoprene and MTs, can capture much of the observed spatial variability in ambient BVOC composition.

The synchronous sampling-period contrasts in ambient MT concentrations provide an additional observational benchmark for model evaluation. Low-latitude forests exhibited daytime MT enhancements that covaried with isoprene, whereas higher-latitude forests showed stronger nighttime MT accumulation. Models can be evaluated against these observed concentration contrasts while accounting for emissions, atmospheric mixing, and chemical loss. The observations do not independently constrain a latitude-dependent change in MT emission light dependence.

The derived oxidant and aerosol-formation metrics also help separate the atmospheric roles of different BVOC classes. Isoprene dominated daytime OFP in broadleaf forests, whereas MTs accounted for 66-97 % of nighttime NO_3 reactivity and more than 70 % of summertime SOAFP (Figs. S15 and S16). MTs and SQTs also contributed substantially to calculated O_3 reactivity. Because these metrics were derived from off-canopy ambient concentrations, they should be interpreted as relative indicators of atmospheric influence rather than as complete in-canopy budgets. Even so, they show that coordinated ambient observations can identify which BVOC classes are most relevant for representing daytime oxidation, nighttime nitrate chemistry, and terpene-driven SOA formation across Chinese forests.

5 Conclusions

This study establishes a coordinated, speciated ambient BVOC benchmark across eight forest and montane ecosystems spanning tropical to cold-temperate China. Using a common sampling and analytical protocol, we compared isoprene, MTs, and SQTs across sites and seasons. The dataset addresses the scarcity of comparable ambient BVOC observations in China and provides a basis for evaluating whether regional models represent BVOC composition and sampling-period variability.

Ambient BVOC composition varied with site context and compound class. Isoprene dominated the measured BVOC mixture at most broadleaf forests, whereas MTs were more prominent at the needleleaf and shrub-steppe sites. Five MTs accounted for most MTs at all sites except QLS, while SQT contributions remained smaller and more site-specific. Winter concentrations tended to be

https://doi.org/10.5194/egusphere-2026-6329
Preprint. Discussion started: 10 November 2026
© Author(s) 2026. CC BY 4.0 License.

lower at paired sites, but the seasonal comparison did not meet the 0.05 significance threshold. Summer daytime isoprene concentrations were higher than nighttime concentrations at all sites, and their associations with air temperature were positive at some, but not all, sites. These observations are consistent with environmental control, but they do not identify emission flux responses because concentrations also reflect light, transport, mixing, and chemical loss.

The calculated reactivity and formation-potential metrics indicate distinct atmospheric roles for the measured BVOC classes. Isoprene contributed most to daytime OH reactivity and OFP at broadleaf sites, whereas MTs contributed strongly to nighttime nitrate-radical reactivity and SOAFP. These are concentration-weighted potentials based on selected ambient compounds, not measurements of complete canopy budgets or realized ozone and aerosol production. Future campaigns should combine continuous vertical ambient measurements with leaf or branch fluxes, leaf temperature, light, and broader chemical coverage. Such observations are needed to separate emission controls from atmospheric processing and to improve BVOC representations in regional chemistry models.

Data availability

The ambient BVOC mixing-ratio datasets in this study are available at https://doi.org/10.5281/zenodo.23392206 (Liu et al., 2026).

Supplement link

The supplement will be linked by Copernicus Publications.

Author contributions

Conceptualization: Yanli Zhang, Xinming Wang. Formal analysis: Di Liu. Funding acquisition: Xinming Wang, Yanli Zhang. Investigation: Junjun Deng, Jianqiang Zeng, Hua Fang, and Zhenfeng Wu. Methodology: Di Liu, Jianqiang Zeng, and Shaoxuan Xiao. Writing - original draft: Di Liu. Writing - review and editing: Pingqing Fu, Yanli Zhang, Ping'an Peng, and Xinming Wang.

Competing interests

The authors declare that they have no conflict of interest.

Acknowledgements

We thank the staff at JFL, XSBN, WYS, SNJ, Qinling Mts. (QL), QLS, CBS, and DXAL, as well as students at the Guangzhou Institute of Geochemistry (Chinese Academy of Sciences) and Tianjin University for their help with air sampling.

Financial support

This work was supported by the National Natural Science Foundation of China (42321003, 41530641, 41673116 and 42673006) and the Department of Science and Technology of Guangdong (2023B1212060049).

References

Arneth, A., Harrison, S. P., Zaehle, S., Tsigaridis, K., Menon, S., Bartlein, P. J., et al. (2010). Terrestrial biogeochemical feedbacks in the climate system. *Nature Geoscience*, *3*, 525-532.

Batista, C. E., Ye, J., Ribeiro, I. O., Guimaraes, P. C., Medeiros, A. S. S., Barbosa, R. G., et al. (2019). Intermediate-scale horizontal isoprene concentrations in the near-canopy forest atmosphere and implications for emission heterogeneity. *Proceedings of the National Academy of Sciences of the United States of America*, *116*, 19318-19323.

https://doi.org/10.5194/egusphere-2026-6329
Preprint. Discussion started: 10 November 2026
© Author(s) 2026. CC BY 4.0 License.

Bourtsoukidis, E., Williams, J., Kesselmeier, J., Jacobi, S., & Bonn, B. (2014). From emissions to ambient mixing ratios: online seasonal field measurements of volatile organic compounds over a Norway spruce-dominated forest in central Germany. *Atmospheric Chemistry and Physics*, *14*, 6495-6510.

Bouvier-Brown, N. C., Goldstein, A. H., Gilman, J. B., Kuster, W. C., & de Gouw, J. A. (2009). In-situ ambient quantification of monoterpenes, sesquiterpenes, and related oxygenated compounds during BEARPEX 2007: implications for gas- and particle-phase chemistry. *Atmospheric Chemistry and Physics*, *9*, 5505-5518.

Chameides, W. L., Lindsay, R. W., Richardson, J., & Kiang, C. S. (1988). The role of biogenic hydrocarbons in urban photochemical smog: Atlanta as a case study. *Science*, *241*, 1473-1475.

Chen, X., Gong, D., Lin, Y., Xu, Q., Wang, Y., Liu, S., et al. (2025). Emission characteristics of biogenic volatile organic compounds in a subtropical pristine forest of southern China. *Journal of Environmental Sciences*, *148*, 665-682.

Claeys, M., Graham, B., Vas, G., Wang, W., Vermeylen, R., Pashynska, V., et al. (2004). Formation of secondary organic aerosols through photooxidation of isoprene. *Science*, *303*, 1173-1176.

Curtius, J., Heinritzi, M., Beck, L. J., Pohlker, M. L., Tripathi, N., Krumm, B. E., et al. (2024). Isoprene nitrates drive new particle formation in Amazon's upper troposphere. *Nature*, *636*, 124-130.

Di Carlo, P., Brune, W. H., Martinez, M., Harder, H., Lesher, R., Ren, X. R., et al. (2004). Missing OH reactivity in a forest: Evidence for unknown reactive biogenic VOCs. *Science*, *304*, 722-725.

Duhl, T. R., Helmig, D., & Guenther, A. (2008). Sesquiterpene emissions from vegetation: a review. *Biogeosciences*, *5*, 761-777.

Edwards, P. M., Evans, M. J., Furneaux, K. L., Hopkins, J., Ingham, T., Jones, C., et al. (2013). OH reactivity in a South East Asian tropical rainforest during the Oxidant and Particle Photochemical Processes (OP3) project. *Atmospheric Chemistry and Physics*, *13*, 9497-9514.

Edwards, P. M., Aikin, K. C., Dube, W. P., Fry, J. L., Gilman, J. B., de Gouw, J. A., et al. (2017). Transition from high- to low-NO_x control of night-time oxidation in the southeastern US. *Nature Geoscience*, *10*, 490-495.

Fang, H., Huang, X., Zhang, Y., Pei, C., Huang, Z., Wang, Y., et al. (2021a). Measurement report: Emissions of intermediate-volatility organic compounds from vehicles under real-world driving conditions in an urban tunnel. *Atmospheric Chemistry and Physics*, *21*, 10005-10013.

Fang, H., Luo, S., Huang, X., Fu, X., Xiao, S., Zeng, J., et al. (2021b). Ambient naphthalene and methylnaphthalenes observed at an urban site in the Pearl River Delta region: Sources and contributions to secondary organic aerosol. *Atmospheric Environment*, *252*, 118295.

Gomes Alves, E., Aquino Santana, R., Quaresma Dias-Júnior, C., Botía, S., Taylor, T., Yáñez-Serrano, A. M., et al. (2023). Intra- and interannual changes in isoprene emission from central Amazonia. *Atmospheric Chemistry and Physics*, *23*, 8149-8168.

Gong, D., Wang, H., Zhang, S., Wang, Y., Liu, S. C., Guo, H., et al. (2018). Low-level summertime isoprene observed at a forested mountaintop site in southern China: implications for strong regional atmospheric oxidative capacity. *Atmospheric Chemistry and Physics*, *18*, 14417-14432.

Guenther, A. B., Jiang, X., Heald, C. L., Sakulyanontvittaya, T., Duhl, T., Emmons, L. K., & Wang, X. (2012). The Model of Emissions of Gases and Aerosols from Nature version 2.1 (MEGAN2.1): an extended and updated framework for modeling biogenic emissions. *Geoscientific Model Development*, *5*, 1471-1492.

Guenther, A. B., Zimmerman, P. R., Harley, P. C., Monson, R. K., & Fall, R. (1993). Isoprene and monoterpene emission rate variability: Model evaluations and sensitivity analyses. *Journal of Geophysical Research: Atmospheres, 98*(D7), 12609–12617.

Guo, H., Ling, Z. H., Cheng, H. R., Simpson, I. J., Lyu, X. P., Wang, X. M., et al. (2017). Tropospheric volatile organic compounds in China. *Science of the Total Environment*, *574*, 1021-1043.

Guo, H., Ling, Z. H., Simpson, I. J., Blake, D. R., & Wang, D. W. (2012). Observations of isoprene, methacrolein (MAC) and methyl vinyl ketone (MVK) at a mountain site in Hong Kong. *Journal of Geophysical Research-Atmospheres*, *117*, D19303.

Heald, C. L., Gouw, J., Goldstein, A. H., Guenther, A. B., Hayes, P. L., Hu, W., et al. (2020). Contrasting reactive organic carbon observations in the Southeast United States (SOAS) and Southern California. *Environmental Science & Technology*, *54*, 14923-14935.

Hellén, H., Praplan, A. P., Tykka, T., Ylivinkka, I., Vakkari, V., Back, J., et al. (2018). Long-term measurements of volatile organic compounds highlight the importance of sesquiterpenes for the atmospheric chemistry of a boreal forest. *Atmospheric Chemistry and Physics*, *18*, 13839-13863.

Hunter, J. F., Day, D. A., Palm, B. B., Yatavelli, R. L. N., Chan, A. W. H., Kaser, L., et al. (2017). Comprehensive characterization

https://doi.org/10.5194/egusphere-2026-6329
Preprint. Discussion started: 10 November 2026
© Author(s) 2026. CC BY 4.0 License.

of atmospheric organic carbon at a forested site. *Nature Geoscience*, *10*, 748-753.

Jardine, K. J., Jardine, A. B., Holm, J. A., Lombardozzi, D. L., Negron-Juarez, R. I., Martin, S. T., et al. (2017). Monoterpene 'thermometer' of tropical forest-atmosphere response to climate warming. *Plant Cell & Environment*, *40*, 441-452.

Jardine, K., Serrano, A. Y., Arneth, A., Abrell, L., Jardine, A., van Haren, J., et al. (2011). Within-canopy sesquiterpene ozonolysis in Amazonia. *Journal of Geophysical Research: Atmospheres*, *116*, D19301.

Jia, Y., Qiao, L., Xie, W., & Li, L. (2024). Spatial-temporal characteristics of ambient isoprene and monoterpene and their ozone and secondary organic aerosol formation potential in China. *Environmental Reviews*, *32*, 203-213.

Jiang, S., Wang, Y., Huang, X., Liu, B., Nie, D., Ge, Y., et al. (2024). Characteristics of nocturnal boundary layer over a subtropical forest: Implications for the dispersion and fate of atmospheric species. *Environmental Science & Technology*, *58*, 23075-23087.

Jones, C. E., Hopkins, J. R., & Lewis, A. C. (2011). In situ measurements of isoprene and monoterpenes within a south-east Asian tropical rainforest. *Atmospheric Chemistry and Physics*, *11*, 6971-6984.

Kesselmeier, J., & Staudt, M. (1999). Biogenic volatile organic compounds (VOC): An overview on emission, physiology and ecology. *Journal of Atmospheric Chemistry*, 33, 23–88.

Kiendler-Scharr, A., Wildt, J., Dal Maso, M., Hohaus, T., Kleist, E., Mentel, T. F., et al. (2009). New particle formation in forests inhibited by isoprene emissions. *Nature*, *461*, 381-384.

Kuhn, U., Rottenberger, S., Biesenthal, T., Wolf, A., Schebeske, G., Ciccioli, P., et al. (2004). Seasonal differences in isoprene and light-dependent monoterpene emission by Amazonian tree species. *Global Change Biology*, *10*, 663-682.

Kurpius, M. R., & Goldstein, A. H. (2003). Gas-phase chemistry dominates O_3 loss to a forest, implying a source of aerosols and hydroxyl radicals to the atmosphere. *Geophysical Research Letters*, *30*, 1371.

Loreto, F., & Sharkey, T. D. (1990). A gas-exchange study of photosynthesis and isoprene emission in *Quercus rubra* L. *Planta*, 182, 523–531.

Laothawornkitkul, J., Taylor, J. E., Paul, N. D., & Hewitt, C. N. (2009). Biogenic volatile organic compounds in the Earth system. *New Phytologist*, *183*, 27-51.

Li, J., Wang, H., Gong, D., Li, Q., Wang, Y., Zhao, W., et al. (2025). Landscape fragmentation triggers cascading enhancement of surface ozone production. *Communications Earth & Environment*, *6*, 931.

Liu, D., Zhang, Y., & Wang, X. (2026). Measurement report: Variability in ambient BVOC compositions along a latitudinal transect of Chinese forests [Dataset]. Zenodo. https://doi.org/10.5281/zenodo.23392206

McFiggans, G., Mentel, T. F., Wildt, J., Pullinen, I., Kang, S., Kleist, E., et al. (2019). Secondary organic aerosol reduced by mixture of atmospheric vapours. *Nature*, *565*, 587-593.

Mermet, K., Sauvage, S., Dusanter, S., Salameh, T., Léonardis, T., Flaud, P.-M., et al. (2019). Optimization of a gas chromatographic unit for measuring biogenic volatile organic compounds in ambient air. *Atmospheric Measurement Techniques*, *12*, 6153-6171.

Nakashima, Y., Kato, S., Greenberg, J., Harley, P., Karl, T., Turnipseed, A., et al. (2014). Total OH reactivity measurements in ambient air in a southern Rocky mountain ponderosa pine forest during BEACHON-SRM08 summer campaign. *Atmospheric Environment*, *85*, 1-8.

Niinemets, Ü., Loreto, F., & Reichstein, M. (2004). Physiological and physicochemical controls on foliar volatile organic compound emissions. *Trends in Plant Science*, 9, 180–186.

Niinemets, U., Monson, R. K., Arneth, A., Ciccioli, P., Kesselmeier, J., Kuhn, U., et al. (2010). The leaf-level emission factor of volatile isoprenoids: caveats, model algorithms, response shapes and scaling. *Biogeosciences*, *7*, 1809-1832.

Nolscher, A. C., Yanez-Serrano, A. M., Wolff, S., de Araujo, A. C., Lavric, J. V., Kesselmeier, J., & Williams, J. (2016). Unexpected seasonality in quantity and composition of Amazon rainforest air reactivity. *Nature Communications*, *7*, 10383.

Ortega, J., Helmig, D., Daly, R. W., Tanner, D. M., Guenther, A. B., & Herrick, J. D. (2008). Approaches for quantifying reactive and low-volatility biogenic organic compound emissions by vegetation enclosure techniques - Part B: Applications. *Chemosphere*, *72*, 365-380.

Palmer, P. I., Marvin, M. R., Siddans, R., Kerridge, B. J., & Moore, D. P. (2022). Nocturnal survival of isoprene linked to formation of upper tropospheric organic aerosol. *Science*, *375*, 562-566.

Peñuelas, J., & Staudt, M. (2010). BVOCs and global change. *Trends in Plant Science*, *15*, 133-144.

https://doi.org/10.5194/egusphere-2026-6329
Preprint. Discussion started: 10 November 2026
© Author(s) 2026. CC BY 4.0 License.

Petersen, R. C., Holst, T., Wu, C., Krejci, R., Chan, J. K., Mohr, C., & Rinne, J. (2025). BVOC and speciated monoterpene concentrations and fluxes at a Scandinavian boreal forest. *Atmospheric Chemistry and Physics*, *25*, 17205-17236.

Pfannerstill, E. Y., Nölscher, A. C., Yáñez-Serrano, A. M., Bourtsoukidis, E., Keßel, S., Janssen, R. H. H., et al. (2018). Total OH reactivity changes over the Amazon rainforest during an El Niño event. *Frontiers in Forests and Global Change*, *1*, 12.

Pfannerstill, E. Y., Reijrink, N. G., Edtbauer, A., Ringsdorf, A., Zannoni, N., Araújo, A., et al. (2021). Total OH reactivity over the Amazon rainforest: variability with temperature, wind, rain, altitude, time of day, season, and an overall budget closure. *Atmospheric Chemistry and Physics*, *21*, 6231-6256.

Ramasamy, S., Ida, A., Jones, C., Kato, S., Tsurumaru, H., Kishimoto, I., et al. (2016). Total OH reactivity measurement in a BVOC dominated temperate forest during a summer campaign, 2014. *Atmospheric Environment*, *131*, 41-54.

Sanchez, D., Seco, R., Gu, D., Guenther, A., Mak, J., Lee, Y., et al. (2021). Contributions to OH reactivity from unexplored volatile organic compounds measured by PTR-ToF-MS - a case study in a suburban forest of the Seoul metropolitan area during the Korea-United States Air Quality Study (KORUS-AQ) 2016. *Atmospheric Chemistry and Physics*, *21*, 6331-6345.

Sarkar, C., Guenther, A. B., Park, J.-H., Seco, R., Alves, E., Batalha, S., et al. (2020). PTR-TOF-MS eddy covariance measurements of isoprene and monoterpene fluxes from an eastern Amazonian rainforest. *Atmospheric Chemistry and Physics*, *20*, 7179-7191.

Scott, C. E., Arnold, S. R., Monks, S. A., Asmi, A., Paasonen, P., & Spracklen, D. V. (2017). Substantial large-scale feedbacks between natural aerosols and climate. *Nature Geoscience*, *11*, 44-48.

Sharkey, T. D., Wiberley, A. E., & Donohue, A. R. (2008). Isoprene emission from plants: why and how. *Annals of Botany*, *101*, 5-18.

Shen, J., Russell, D. M., DeVivo, J., Kunkler, F., Baalbaki, R., Mentler, B., et al. (2024). New particle formation from isoprene under upper-tropospheric conditions. *Nature*, *636*, 115-123.

Shrivastava, M., Andreae, M. O., Artaxo, P., Barbosa, H. M. J., Berg, L. K., Brito, J., et al. (2019). Urban pollution greatly enhances formation of natural aerosols over the Amazon rainforest. *Nature Communications*, *10*, 1046.

Sinha, V., Williams, J., Lelieveld, J., Ruuskanen, T. M., Kajos, M. K., Patokoski, J., et al. (2010) OH reactivity measurements within a boreal forest: Evidence for unknown reactive emissions. *Environmental Science & Technology*, *44*, 6614-6620.

Staudt, M., & Bertin, N. (1998). Light and temperature dependence of the emission of cyclic and acyclic monoterpenes from holm oak (*Quercus ilex* L.) leaves. *Plant, Cell & Environment*, 21, 385–395.

Su, Y., Guo, Q., Hu, T., Guan, H., Jin, S., An, S., et al. (2020). An updated vegetation map of China (1:1000000). *Science Bulletin*, *65*, 1125-1136.

Wang, N., Huang, X., Xu, J., Wang, T., Tan, Z.-M., & Ding, A. (2022). Typhoon-boosted biogenic emission aggravates cross-regional ozone pollution in China. *Science Advances*, *8*, eabl6166.

Weber, J., King, J. A., Abraham, N. L., Grosvenor, D. P., Smith, C. J., Shin, Y. M., et al. (2024). Chemistry-albedo feedbacks offset up to a third of forestation's CO_2 removal benefits. *Science*, *383*, 860-864.

Xu, L., Guo, H., Boyd, C. M., Klein, M., Bougiatioti, A., Cerully, K. M., et al. (2015). Effects of anthropogenic emissions on aerosol formation from isoprene and monoterpenes in the southeastern United States. *Proceedings of the National Academy of Sciences of the United States of America*, *112*, 37-42.

Xue, L. K., Wang, T., Guo, H., Blake, D. R., Tang, J., Zhang, X. C., et al. (2013). Sources and photochemistry of volatile organic compounds in the remote atmosphere of western China: results from the Mt. Waliguan Observatory. *Atmospheric Chemistry and Physics*, *13*, 8551-8567.

Yáñez-Serrano, A. M., Nölscher, A. C., Bourtsoukidis, E., Gomes Alves, E., Ganzeveld, L., Bonn, B., et al. (2018). Monoterpene chemical speciation in a tropical rainforest: variation with season, height, and time of day at the Amazon Tall Tower Observatory (ATTO). *Atmospheric Chemistry and Physics*, *18*, 3403-3418.

Yang, X., Wang, H., Lu, K., Ma, X., Tan, Z., Long, B., et al. (2024). Reactive aldehyde chemistry explains the missing source of hydroxyl radicals. *Nature Communications*, *15*, 1648.

Zannoni, N., Leppla, D., Lembo Silveira de Assis, P. I., Hoffmann, T., Sá, M., Araújo, A., & Williams, J. (2020). Surprising chiral composition changes over the Amazon rainforest with height, time and season. *Communications Earth & Environment*, *1*, 4.

Zannoni, N., Gros, V., Lanza, M., Sarda, R., Bonsang, B., Kalogridis, C., et al. (2016). OH reactivity and concentrations of biogenic volatile organic compounds in a Mediterranean forest of downy oak trees. *Atmospheric Chemistry and Physics*, *16*, 1619-1636.

Zeng, J., Zhang, Y., Mu, Z., Pang, W., Zhang, H., Wu, Z., et al. (2023). Temperature and light dependency of isoprene and

https://doi.org/10.5194/egusphere-2026-6329
Preprint. Discussion started: 10 November 2026
© Author(s) 2026. CC BY 4.0 License.

monoterpene emissions from tropical and subtropical trees: Field observations in south China. *Applied Geochemistry*, *155*, 105727.

Zeng, J., Zhang, Y., Pang, W., Ran, H., Mu, Z., Guo, H., et al. (2025a). Contrasting Emission seasonality between light-dependent and light-independent biogenic VOCs from subtropical Eucalyptus trees. *Journal of Geophysical Research: Atmospheres*, *130*, e2025JD043387.

Zeng, J., Zhang, Y., Pang, W., Ran, H., Guo, H., Lu, Y., et al. (2025b). Heatwaves suppress isoprene emission optima in subtropical Eucalyptus: Implications for biogenic VOC modeling under extreme thermal events. *Geophysical Research Letters*, *52*, e2025GL114767.

Zeng, J., Zhang, Y., Pang, W., Ran, H., Mu, Z., Guo, H., et al. (2025c). Decoupling temperature and light effects on terpene emissions from subtropical Eucalyptus: Insights from controlled field experiments. *Journal of Geophysical Research: Atmospheres*, *130*, e2024JD042616.

Zeng, J., Zhang, Y., Ran, H., Pang, W., Guo, H., Mu, Z., et al. (2025d). Calibrating adsorptive and reactive losses of monoterpenes and sesquiterpenes in dynamic chambers using deuterated surrogates. *Atmospheric Measurement Techniques*, *18*, 1811-1821.

Zeng, J., Zhang, Y., Zhang, H., Song, W., Wu, Z., & Wang, X. (2022). Design and characterization of a semi-open dynamic chamber for measuring biogenic volatile organic compound (BVOC) emissions from plants. *Atmospheric Measurement Techniques*, *15*, 79-93.

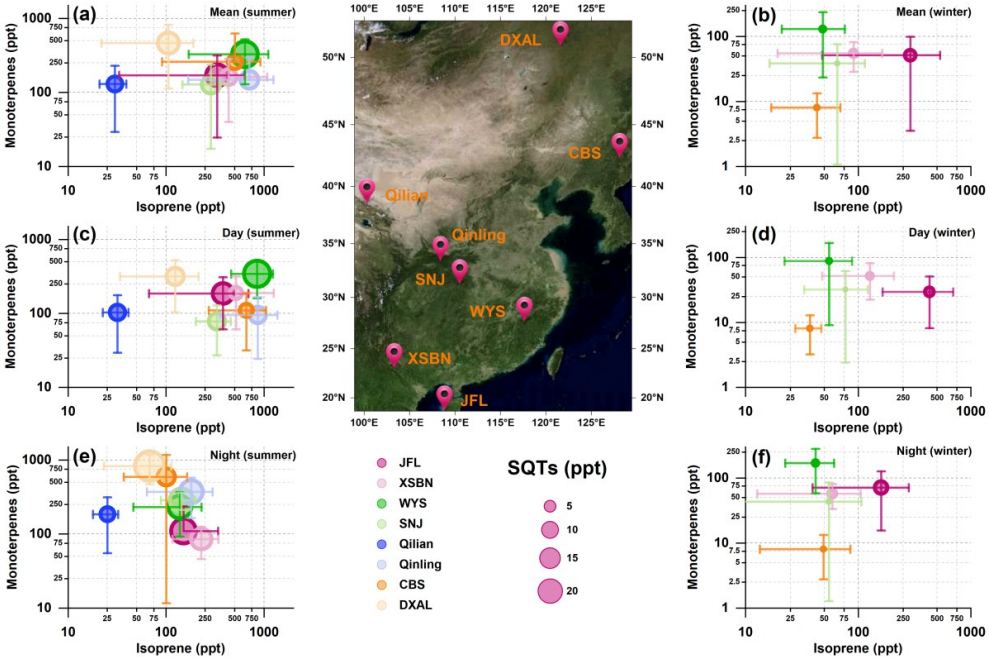
Zhang, Y., Zhang, R., Yu, J., Zhang, Z., Yang, W., Zhang, H., et al. (2020). Isoprene mixing ratios measured at twenty sites in China during 2012-2014: Comparison with model simulation. *Journal of Geophysical Research: Atmospheres*, 125, e2020JD033523.

Zhang, Y., Men, Y., Guo, H., Shen, G., Gao, Y., Xiong, R., et al. (2025). Combustion-related isoprene contributes substantially to the formation of wintertime secondary organic aerosols. *National Science Review*, 12, nwae474

Zhang, Y., Cui, S., Li, J., Wang, M., Xu, X., Wang, J., et al. (2026). Urban black-carbon radiative heating intensified by biogenic-anthropogenic interactions. *Nature Geoscience*, *19*, 439-446.

Zhao, B., Donahue, N. M., Zhang, K., Mao, L., Shrivastava, M., Ma, P. L., et al. (2024). Global variability in atmospheric new particle formation mechanisms. *Nature*, *631*, 98-105.

https://doi.org/10.5194/egusphere-2026-6329
Preprint. Discussion started: 10 November 2026
© Author(s) 2026. CC BY 4.0 License.



545 **Figure 1.** Overview of mixing ratios of isoprene, monoterpenes, and sesquiterpenes at eight Chinese forest sites in summer (a, c, e) and winter (b, d, f), 2019. Panels (a, b) show means for the sampled periods, (c, d) daytime means, and (e, f) nighttime means. Isoprene and MT mixing ratios are shown on the horizontal and vertical axes, respectively; circle size indicates the SQT mixing ratio. Error bars represent standard deviations.

https://doi.org/10.5194/egusphere-2026-6329
Preprint. Discussion started: 10 November 2026
© Author(s) 2026. CC BY 4.0 License.

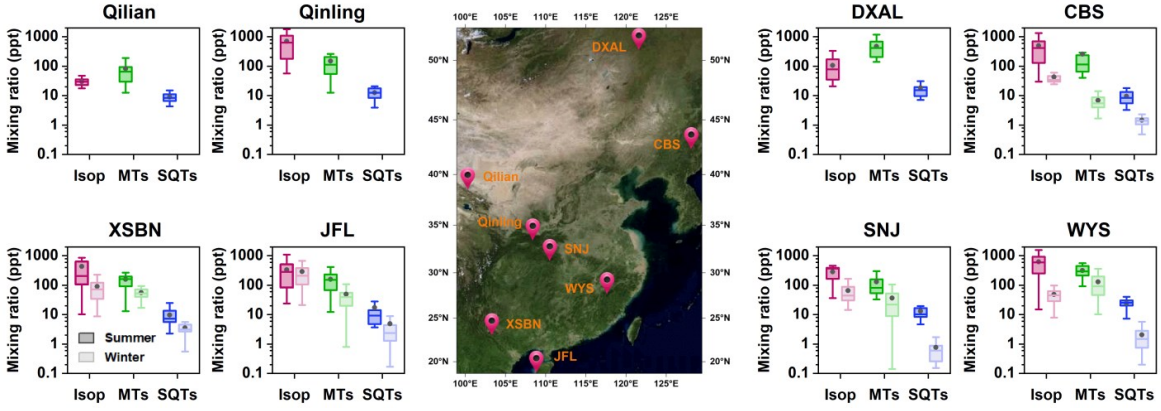
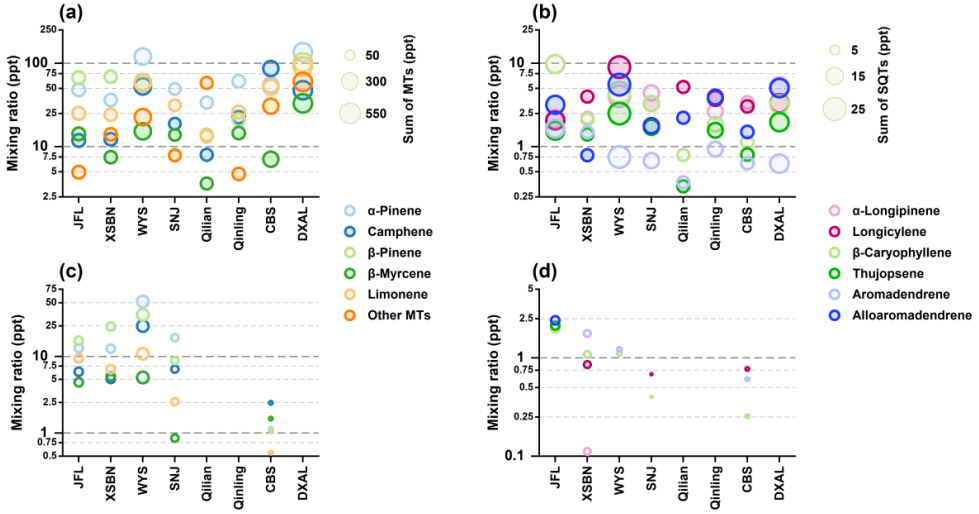


Figure 2. Spatial and seasonal variation of mixing ratios of isoprene (Isop), monoterpenes (MTs), and sesquiterpenes (SQTs) at eight Chinese forest sites.

https://doi.org/10.5194/egusphere-2026-6329
Preprint. Discussion started: 10 November 2026
© Author(s) 2026. CC BY 4.0 License.



555 **Figure 3.** Monoterpene and sesquiterpene mixing ratios and compositions of different forests in summer (a, b) and winter (c, d), 2019. Other MTs include 3-carene, α-phellandrene, 1,8-cineole, γ-terpinene, terpinolene, linalool, and α-terpinene.

https://doi.org/10.5194/egusphere-2026-6329
Preprint. Discussion started: 10 November 2026
© Author(s) 2026. CC BY 4.0 License.

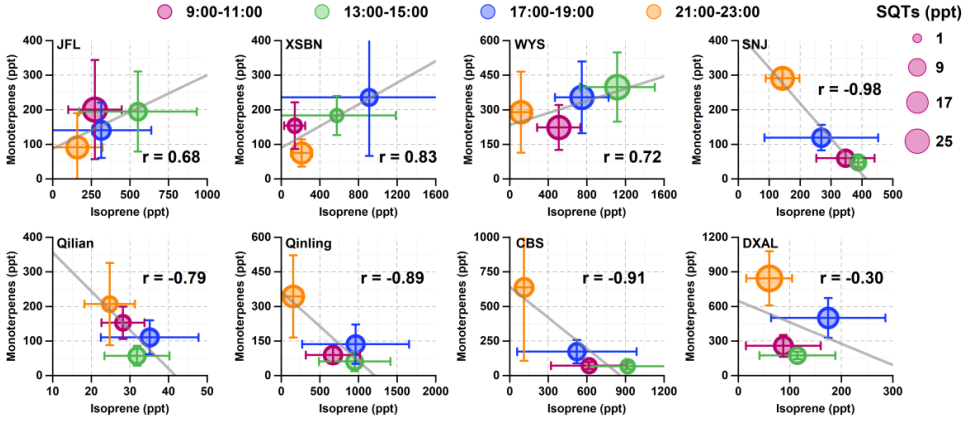


Figure 4. Correlation between isoprene and monoterpene mixing ratios at the four fixed sampling periods in summer. Each point represents a sampling-period mean. Error bars represent standard deviations, while circle size indicates sesquiterpene mixing ratio.

https://doi.org/10.5194/egusphere-2026-6329
Preprint. Discussion started: 10 November 2026
© Author(s) 2026. CC BY 4.0 License.

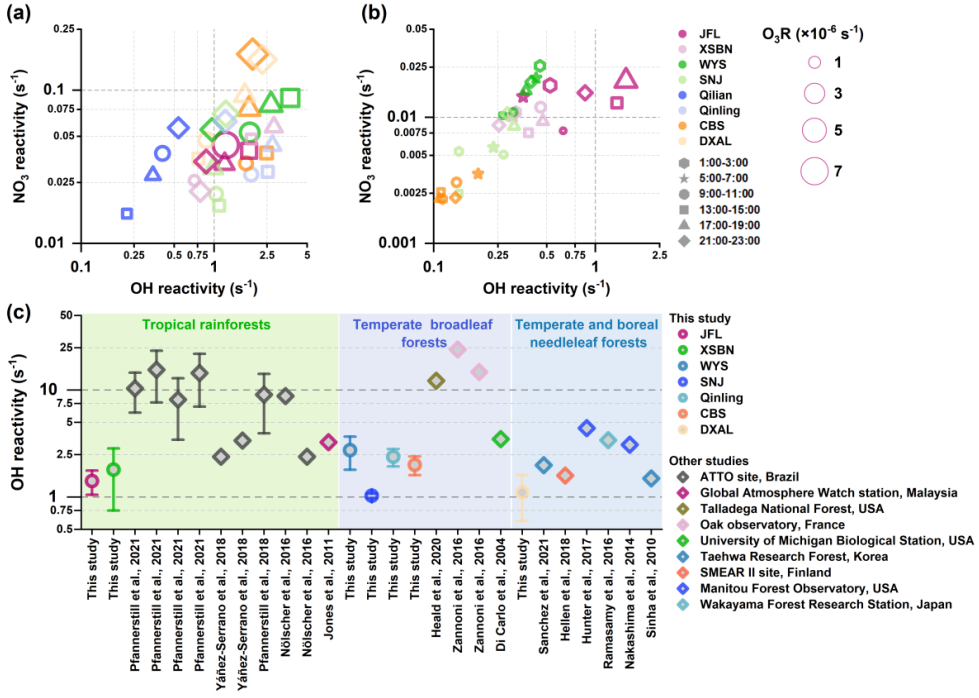
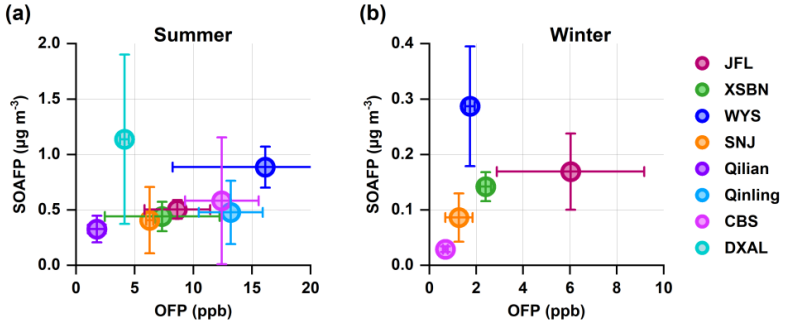


Figure 5. Calculated oxidant reactivity for different forests at each sampling period in summer (a) and winter (b), respectively. Comparison of calculated OH reactivity from the measured isoprenoids in this study with calculated reactivities for the compound sets reported in Table S5 (c). Error bars represent standard deviations.

https://doi.org/10.5194/egusphere-2026-6329
Preprint. Discussion started: 10 November 2026
© Author(s) 2026. CC BY 4.0 License.



570 **Figure 6.** Calculated ozone and SOA formation potential for different forests in summer (a) and winter (b).

https://doi.org/10.5194/egusphere-2026-6329
Preprint. Discussion started: 10 November 2026
© Author(s) 2026. CC BY 4.0 License.

Table 1. BVOC mixing ratios (mean ± s.d.) at different forests and seasons.

Forest sites	Season	Isoprene (ppt)	MTs (ppt)	SQTs (ppt)
JFL	Summer	332±299	172±147	20±38
	Winter	289±242	52±48	7±10
XSBN	Summer	434±641	164±124	12±10
	Winter	91±71	56±27	4±2
WYS	Summer	639±469	329±199	27±13
	Winter	48±27	131±107	2±2
SNJ	Summer	286±139	129±112	15±10
	Winter	65±49	39±38	1±1
CBS	Summer	503±412	261±371	11±7
	Winter	43±26	8±5	2±1
QL	Summer	709±540	150±150	15±8
QLS	Summer	30±9	131±101	11±5
DXAL	Summer	106±84	470±356	19±14